34th Annual International Conference of the IEEE EMBS
San Diego, California USA, 28 August - 1 September, 2012

An *in-vivo* computed tomography approach for quantifying porcine pulmonary arterial morphometry.*

Yik Ching Lee[1], Alys Clark[1], Matthew Fuld[3], Susan Haynes[2], Abhay Divekar[2, 3], Eric Hoffman[3, 4], Merryn Tawhai[1]

[1]*Auckland Bioengineering Institute, The University of Auckland, 92019 Auckland, New Zealand; Departments of* [2]*Deparment of Pediatrics, Division of Pediatric Cardiology ,*[3]*Radiology,* [4]*Biomedical Engineering, University of Iowa, Iowa City, Iowa 52242*

***Abstract*— the objective of this study was to develop an *in vivo* CT imaging-based approach for pulmonary arterial morphometry measurement, and to improve the geometrical basis for studies of the porcine vasculature. The luminal diameter and distance from the inlet of left and right pulmonary arteries, and pulmonary arteries within the lungs of two porcine subjects were measured at inflation pressure of 25 cmH_2O. The results suggest that the porcine pulmonary arteries have geometric self-similarity, and that this approach will have utility for systematically quantifying pulmonary arterial vessel dimensions *in vivo* in a larger group of animals.**

I. Introduction

The structure of the pulmonary vasculature plays a significant role in determining the distribution of pulmonary perfusion [1], and hence this affects the lung's response to disease. Porcine models are often used in experimental studies that are aimed at improving understanding of human disorders. Pigs have shown significant advantages over smaller animals because of their physiological and anatomical similarity to man, which permits a variety of clinical scenarios to be simulated. A quantitative description of the porcine pulmonary vasculature is therefore essential to understanding structure-function relationships in this species, and how this translates to the human lung. However, knowledge on morphometry of the pig pulmonary vasculature remains rudimentary.

Previous studies describing the morphometry of the porcine pulmonary circulation are few in number, and they lack detailed geometric information. The most extensive morphological study was conducted by Maina et al. [2], who measured the size of arteries over 22 generations of silicone elastomer casts of the right lungs of two pigs. Data were presented as means per generation, which groups together arteries of dissimilar size because ordering by generation neglects tree asymmetry. Casting is a painstaking process that cannot be repeated on large numbers of animals. Rendas et al. [3] conducted a morphometric analysis on the postnatal development of the pig lung, however the geometric details were not fully described. Other previous studies have used microfocal computed tomography (micro-CT) to examine morphometry and self-similarity in the rat pulmonary arteries [4], and multi-detector row computed tomography (MDCT) to quantify the geometry of the human and ovine bronchial airways [5]. Such rapid imaging allows for *in vivo* measurement of geometry and can be readily performed on many subjects. Here we propose a similar approach to these previous studies to quantify the porcine pulmonary arteries using MDCT imaging of the intact lung. We propose a simple and rapid method for estimating artery diameter, and examine whether the porcine pulmonary arteries exhibit self-similarity.

*Research supported by Health Research Council of New Zealand grant HRC-09/143.

Address correspondence to Merryn Tawhai, Auckland Bioengineering Institute, The University of Auckland, Private Bag 92019, Auckland, New Zealand (phone: +64 9 373 7599 ext: 85119; e-mail: m.tawhai@auckland.ac.nz).

II. Material and Methods

A. Animal Preparation and Imaging

In vivo imaging was conducted at the University of Iowa I-CLIC (Iowa Comprehensive Lung Imaging Center) following approval by the University of Iowa Institutional Animal Care and Use Committee. One healthy pig of each gender was used in this initial study (21 kg female and 40 kg male). Animals were pre-medicated with 20 mg/kg Ketamine and 2 mg/kg Xylazine intramuscularly (IM) and anesthetized with 1 - 3 % Isoflurane via nose cone inhalation. Anaesthesia was maintained with continuous intravenous (IV) administration of Pentobarbital (0-30 mg/kg loading, 3-5 mg/kg/hr maintenance). Pancuronium was administered at 2.5 mg initially, 0.5-1.0 mg as needed. Tracheostomy was performed and the animals were mechanically ventilated with 100% oxygen for the duration of the study. The animals were in the prone position for volume scans which were acquired during breath-hold at an inflation pressure of 25 cmH_2O.

Volume scans were obtained using a dual source CT scanner (Siemens Medical Systems, Erlangen, Germany), whereby two x-ray guns serve to double the temporal resolution of the scanner system [6]. The animals were imaged during a breath hold using a retrospective cardiac gating method with an image resolution of 0.51 mm/pixel, and slice thickness of 0.5 mm.

B. Measurements

The geometric measurement algorithm is described in Figure 1. First the vasculature was extracted from the imaging data using the custom-written software Pulmonary Analysis Software Suite (PASS, University of Iowa) [7, 8]. A three dimensional rendering of these blood vessels in a single animal are shown in Figure 2A. Arteries and vein were then manually distinguished from each other, using the PASS segmented airway tree as a guide (arteries accompany the airways and branch with them, and veins are found in between the airways).

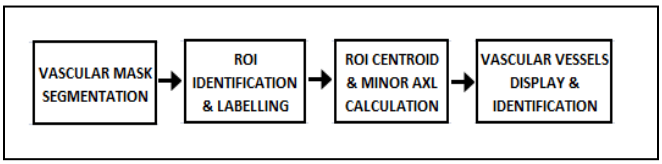

Figure 1. Flowchart of geometric measurement algorithm

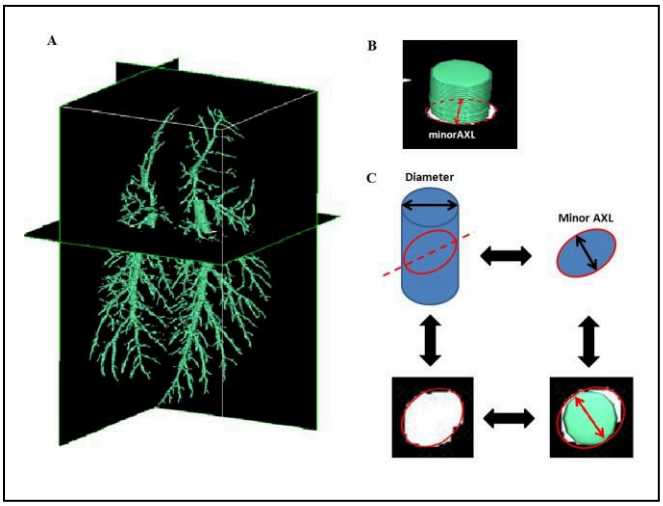

Figure 2. A. Three-dimensional rendering of a porcine pulmonary arterial tree. B. Segmented vascular vessel mask slice with its elliptical cross-section of the vessel due to the oblique angle between the vessel segment central axis and the imaging system axis of rotation (with minor axis length indicated). C. Schematic representation of minor AXL is equivalent to the diameter of the vascular vessel.

Segmented vessel masks were imported into MATLAB® in sequential order. Each individual mask slice was then represented as a 512×512 matrix in binary format. The blood vessels in each slice were assigned a pixel value of 1 and other material (lung parenchyma, bone, air) was assigned a pixel value of zero. Each blood vessel region (a cluster of pixels with value 1) was then labelled as a region of interest (ROI). The elliptical cross section, its centroid, and its minor axis length were then calculated using the MATLAB function 'regionprops'. Each ROI was then characterised by these measures with x and y coordinates identified by pixel number, and z coordinate identified by slice number. The minor axis length of an ROI is equivalent to the diameter of the vessel, assuming that the vessel is approximately circular in cross section (see Figure 2B and C). The data describing the vascular tree structure (containing centroid location and minor axis length (i.e. diameter) were then imported into the CMGUI visualization software (www.cmiss.org/cmgui, University of Auckland), and used for 3D visualization and quantitative structural assessment. The ROIs corresponding to each blood vessel were manually identified in CMGUI. Each blood vessel segment was then associated with diameters and centreline locations for analysis.

The left and right pulmonary arteries that branch out from the main pulmonary artery were identified manually (Figure 3A). The main pulmonary artery that connects the pulmonary vasculature to the heart cannot be easily distinguished due to the lack of contrast in the MDCT scans.

C. Data analysis

Because this study utilizes an *in vivo* approach, identification of the complete arterial tree cannot be guaranteed. That is, some arteries may have given rise to small arteries that were not adequately resolved on the imaging and hence are missing from our data. We therefore present the following results as diameter variation with distance along selected arterial pathways, and geometry metrics calculated at the branch divisions.

III. RESULTS

Figure 3A indicates the location of the left and right principal pathways that were used in the initial analysis. The distance from the pathway inlet to each ROI (diameter measurement) location is plotted against vessel diameter in Figure 3B. For both the left and right main pathways of both the animals, the diameter versus distance relationship followed a clear trend of decreasing diameter with distance from the tree inlet. Linear relationships (shown in Figure 3B) and curved relationships [4, 9] were fit to the data. Linear relationships provided good fits to each data set ($R^2 > 0.93$ in each case). The R^2 for the curved fits (negative exponential) was smaller in each case than for the linear fit. An F-ratio test showed that the linear fits were better fits to the data in each case at the 95% confidence level.

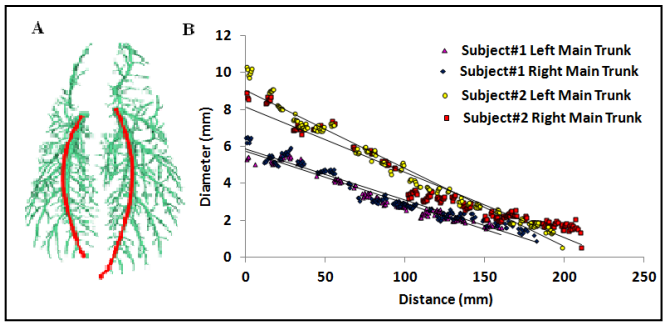

Figure 3. A: Rendering of a pig pulmonary arterial tree, with left and right main arterial pathways highlighted. B: Diameter (mm) versus distance (mm) relationships for the left and right main arteries of two animals.

To determine whether there is a similar relationship between diameter and pathlength when animal size is accounted for, the data were normalized by the path's inlet diameter and shifted to a common start point. The normalized data for the four arterial pathways showed similar decrease in normalized diameter with normalized distance from the pathway inlet (mean -0.81 ± 0.03; range -0.78 to -0.84). Comparison of each data set (using a t-test with significance level of 5%) showed no statistically significant difference between the four slopes.

To evaluate whether the arterial tree exhibits self-similarity, five additional pathways from each animal were measured as indicated in Figure 4A. The data from these pathways are superimposed on the main pathway in Figure 4B, illustrating their similarity when distance from the main pathway inlet is taken into account. Inclusion of these data did not change the linear fit.

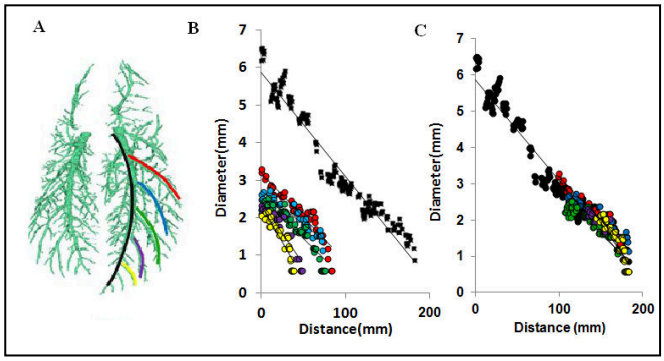

Figure 4. A: Six arterial pathways from which data was acquired and identified by colored lines. B: Diameter versus distance relationships for the six individual pathways.C: superposition of the 5 minor arteries on the main artery by shifting the distance axis.

Summary geometry statistics were calculated on the total pooled data. Because the measurement of individual artery length depends on identifying all child arteries that arise from the branch, here we present only those metrics that are independent of length. Previous cast-based studies did not report these metrics, so we include (italicised, in brackets) data from the ovine airway tree for comparison [5]. A total of 1148 arteries (pooled for the two animals) were analyzed. The angle between a parent and child branch was 37.14 ± 21.84° (*35.88 ± 22.32°*); the angle between a parent and its major or minor child branch was 24.53 ± 18.19° (*25.17 ± 16.85°*) and 47.31 ± 20.47° (*45.99 ± 21.94°*), respectively. The angle of rotation between branching planes was 87.08 ± 47.33° (*89.04 ± 44.64°*). The ratio of child to parent diameter was 0.70 ± 0.25 (*0.71 ± 0.18*); the same ratio for major and minor child branches was 0.85 ± 0.21 (0.86 ± *0.12*) and 0.56 ± 0.19 (0.61 ± *0.12*), respectively. Comparison of each data set with known sample sizes, mean values and standard deviation (using a t-test with significance level of 5%) showed that the mean geometric values of both species were not significantly different from each other.

IV. CONCLUSIONS

This initial study on two animals suggests that the porcine pulmonary arteries show properties of self-similarity, such that any pathway in the tree can be geometrically defined by measuring any other pathway. If this finding holds with the addition of more animals to the study, then this is consistent with previous studies in rat [4]. The data further suggests that the rate of reduction of diameter with distance from the arterial tree inlet is similar between individual pigs, when differences in overall vascular tree size are accounted for.

The angle between planes of branching ('rotation angle') has been measured to be close to 90° in other animal species [10], which is consistent with our data. Our branching angles and diameter ratios were similar to values reported for the ovine airway tree [5]. This comparison between ovine and porcine lung anatomies suggests that our data is consistent with other quadruped morphometry, and that the ovine and porcine pulmonary trees are similar in some aspects of their geometry.

Our data were acquired at a single airway inflation pressure. This potentially affects the magnitude of the artery diameters and lengths, but is unlikely to affect the proportionality between parent and child diameters, or branching angles, because the lung is affected similarly throughout. While our data acquisition method cannot be guaranteed to capture all arteries that would be necessary for a description of geometry by generation, the method is sufficient for analysis by distance from inlet. Our initial results suggest that – because of self-similarity - this is sufficient to define the geometry of the entire arterial tree. The addition of data from more animals will strengthen these conclusions.

ACKNOWLEDGMENTS

This work was supported by Health Research Council of New Zealand grant HRC 09-143.

REFERENCES

[1] K. S. Burrowes, E. A. Hoffman, and M. H. Tawhai, "Species-Specific Pulmonary Arterial Asymmetry Determines Species Differences in Regional Pulmonary Perfusion " *Annals of Biomedical Engineering,* vol. 37, pp. 2497-2509, 2009.

[2] J. N. Maina and P. v. Gils, "Morphometric chracaterization of the airway and vascular systems of the lung of the domestic pig, Sus scrofa: comparison of the airway, arterial and venous systems," *Comparative Biochemistry and Physiology,* p. 18, 2001.

[3] A. Rendas, B. M., and L. Reid, "Growth of pulmonary circulation in normal pig - structural analysis and cardiopulmonary function.," *Journal of Applied Physiology - Respiratory, Environmental and Exercise Physiology,* vol. 45, pp. 806-817, 1978.

[4] K. L. Karau, R. H. Johnson, R. C. Molthen, A. H. Dhyani, S. T. Haworth, C. C. Hanger, D. L. Roerig, and C. A. Dawson, "Microfocal X-ray CT imaging and pulmonary arterial

distensibility in excised rat lungs," *American Journal of Physiology - Heart Circulatory Physiology,* vol. 281, pp. H1447-H1457, 2001.

[5] M. H. Tawhai, P. J. Hunter, J. Tschirren, J. M. Reinhardt, G. McLennan, and E. A. Hoffman, "CT-based geometry analysis and finite element models of the human and ovine bronchial tree," *Journal of Applied Physiology,* vol. 97, pp. 2310-2321, 2004.

[6] E. A. Hoffman, B. A. Simon, and G. McLennan, "A Structural and Functional Assessment of the Lung via Multidetector-Row Computed Tomography - Phenotyping Chronic Obstructive Pulmonary Disease," 2006, pp. 519–534.

[7] E. A. Hoffman, A. V. Clough, G. E. Christensen, C. L. Lin, G. McLennan, J. M. Reinhardt, B. A. Simon, M. Sonka, M. H. Tawhai, E. J. van Beek, and G. Wang, "The comprehensive imaging-based analysis of the lung: a forum for team science.," *Academic Radiology,* vol. 11, pp. 1370-1380, 2004.

[8] S. Hu and E. A. Hoffman, "Automatic lung segmentation for accurate quantitation of volumetric X-ray CT images," *IEEE Transactions on Medical Imaging,* vol. 20, pp. 490-498, 2001.

[9] K. L. Karau, R. C. Molthen, A. Dhyani, S. T. Haworth, C. C. Hanger, D. L. Roerig, R. H. Johnson, and C. A. Dawson, "Pulmonary arterial morphometry from microfocal X-ray computed tomography," *American Journal of Physiology - Heart Circulatory Physiology,* vol. 281, pp. H2747-H2756 2001.

[10] K. Horsfield, "Anatomical factors influencing gas mixing and distribution.," in *Gas Mixing and Distribution in the Lung (Lung Biology in Health and Disease)*, L. A. Engel and M. Paiva, Eds., ed: Informa Healthcare, 1985.